

Receding Horizon Motion Planning for Multi-Agent Systems: A Velocity Obstacle Based Probabilistic Method

Xiaoxue Zhang, Jun Ma, Zilong Cheng, Sunan Huang, and Tong Heng Lee

Abstract—In this paper, a novel and innovative methodology for feasible motion planning in the multi-agent system is developed. On the basis of velocity obstacles characteristics, the chance constraints are formulated in the receding horizon control (RHC) problem, and geometric information of collision cones is used to generate the feasible regions of velocities for the host agent. By this approach, the motion planning is conducted at the velocity level instead of the position level. Thus, it guarantees a safer collision-free trajectory for the multi-agent system, especially for the systems with high-speed moving agents. Moreover, a probability threshold of potential collisions can be satisfied during the motion planning process. In order to validate the effectiveness of the methodology, different scenarios for multiple agents are investigated, and the simulation results clearly show that the proposed approach can effectively avoid potential collisions with a collision probability less than a specific threshold.

Index Terms—Receding horizon control, motion planning, multi-agent systems, chance constraints, velocity obstacle.

I. INTRODUCTION

Motion planning is one of the essential components of intelligent robots, and an efficient trajectory can effectively improve robots' intelligence and autonomy [1], [2]. The velocity obstacles approach is a geometry-based method that defines conic regions as constraints on the feasible velocities for agents. The concepts of collision cones and velocity obstacles approach are introduced in [3]. This kind of method can be used to find the range of feasible velocity quickly with minimal obstacle information without any prior knowledge or prediction, after given the collision scenario geometrically [4]. There are several variants of the velocity obstacles approach, i.e., reciprocal velocity obstacles [5], accelerated velocity obstacles [6], generalized velocity obstacles [7], hybrid reciprocal velocity obstacles [8], etc. However, most of these variants consider the feasible velocity direction with neglecting the optimality of the planned trajectory.

In order to find a feasible velocity based on the collision region provided by velocity obstacles, receding horizon control

(RHC), which is also known as model predictive control (MPC), can be utilized to find the optimal velocity and position [9]. It is one typical effective approach that has been widely applied in the decision making, planning, and control of robots [10]–[12]. MPC has the capability of addressing various constraints as part of the control synthesis problem [13]–[16]. In terms of the uncertainties of path planning, one can characterize these uncertainties in a probabilistic manner and find the optimal sequence of control inputs subject to the chance constraints, which means that the probability of collision avoidance should not be lower than a user-defined threshold [17]–[19]. Such a probabilistic approach has multiple advantages compared to the traditional box constraints approach, as most of the uncertainties can be represented by a stochastic model instead of a bounded set [20]. Besides, the probability threshold will influence the conservatism of the planned trajectory. A proper probability threshold can balance conservatism and performance. There are a number of previous works regarding the chance constrained path planning with the existence of obstacles [21]–[24]. However, most of the existing probabilistic approaches still stay on the position-based level to achieve motion planning, which means the position information is mainly utilized to make a decision. Thus, these approaches at the position-based level could not be suitable even valid in some scenes, especially in fast-moving scenarios.

This paper presents a novel approach to plan the optimal trajectories for the multi-agent system through the confinement of collision probability, based on the information of velocity obstacles. This approach generates a feasible region of velocity for the host agent when computing an optimal trajectory. Then the feasible region is further formulated as probabilistic collision constraints. This method is capable of planning the trajectories at the velocity level, which is much more meaningful than the traditional counterpart at the position level, especially effective for the scenarios with high-speed obstacles. Also, a collision probability can be confined within a specific range in the proposed approach. The structure of this paper is as follows. In Section II, the basic concept and definitions of the velocity obstacles method are introduced. Section III formulates the chance constrained receding horizon optimization problem based on the velocity obstacles. In Section IV, we transform the probabilistic constraints in the model predictive control (MPC) problem into deterministic constraints and then solve this problem by multiple shooting method. Section V shows the simulation results in different

X. Zhang, Z. Cheng, and T. H. Lee are with the NUS Graduate School for Integrative Sciences and Engineering, National University of Singapore, Singapore 119077 (e-mail: xiaoxuezhang@u.nus.edu; zilongcheng@u.nus.edu; eleleeth@nus.edu.sg).

J. Ma is with the Department of Mechanical Engineering, University of California, Berkeley, CA 94720 USA (e-mail: jun.ma@berkeley.edu).

S. Huang is with the Temasek Laboratories, National University of Singapore, Singapore, 117411 (e-mail: tslhs@nus.edu.sg).

This work has been submitted to the IEEE for possible publication. Copyright may be transferred without notice, after which this version may no longer be accessible

scenarios, and conclusion is presented in Section VI.

II. VELOCITY OBSTACLES

In this section, the basic concept of the velocity obstacles approach is introduced, and the geometric illustration is shown in Fig. 1. The related parameters and variables in this figure are explained below.

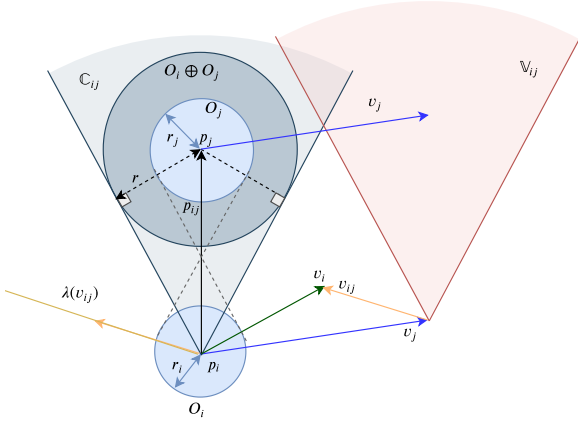


Fig. 1. Velocity obstacles

Let all circular moving objects O_i and O_j be centered at $p_i \in \mathbb{R}^n$ and $p_j \in \mathbb{R}^n$ with radius r_i and r_j and velocities $v_i \in \mathbb{R}^n$ and $v_j \in \mathbb{R}^n$, respectively, where

$$\begin{aligned} O_i &= \{p_i + \mu r_i \mid \|\mu\|_2 \leq 1\} \\ O_j &= \{p_j + \mu r_j \mid \|\mu\|_2 \leq 1\}. \end{aligned} \quad (1)$$

Let \oplus denotes the Minkowski sum operation, and we have

$$O_i \oplus O_j = \{m_i + m_j \mid m_i \in O_i, m_j \in O_j\}. \quad (2)$$

The relative velocity between i th object and j th object is $v_{ij} := v_i - v_j$. Let $\lambda(v_{ij})$ denote the ray with direction v_{ij} from the position p_i , where

$$\lambda(v_{ij}) = \{p_i + \lambda v_{ij} \mid \lambda \geq 0\}. \quad (3)$$

Then the object i and the object j will collide if and only if

$$\lambda(v_{ij}) \cap (O_i \oplus O_j) \neq \emptyset. \quad (4)$$

Therefore, a collision cone \mathbb{C}_{ij} can be represented by

$$\mathbb{C}_{ij} = \{v_{ij} \mid (O_i \oplus O_j) \cap \lambda_{ij}(v_{ij}) \neq \emptyset\}. \quad (5)$$

In order to determine whether the velocity v_i of the i th object has a risk of collision with the j th object, the velocity obstacle \mathbb{V}_{ij} is defined as

$$\mathbb{V}_{ij} = \{v_i \mid (v_i - v_j) \in \mathbb{C}_{ij}\}, \quad (6)$$

which is equivalent to

$$\mathbb{V}_{ij} = v_j + \mathbb{C}_{ij}, \quad (7)$$

for the i th object. Any velocity $v_i \in \mathbb{V}_{ij}$ will result in a collision, as shown in Fig. 1.

The set of all moving surrounding objects can be considered as obstacles for the host object i . Assume the set of all moving objects is $\mathbb{N}_n = \{1, 2, \dots, n\}$. The composite velocity obstacles and collision cones are

$$\begin{aligned} \mathbb{V}_i &= \cup_{j \neq i} \mathbb{V}_{ij} \\ \mathbb{C}_i &= \cup_{j \neq i} \mathbb{C}_{ij}. \end{aligned} \quad (8)$$

III. PROBLEM STATEMENT

A. Objects Model and Collision Chance Constraints

1) *Objects Model*: The dynamics of each planar object $i \in \mathbb{N}_n$ can be represented by any stochastic nonlinear or linear, continuous-time or discrete-time model, where

$$\dot{x}_i = f_i(x_i, u_i) + \omega_i \quad \text{or} \quad x_i^{k+1} = g_i(x_i^k, u_i^k) + \omega_i^k, \quad (9)$$

where $x_i = [p_i^T, v_i^T]^T \in \mathcal{X}_i \subset \mathbb{R}^{n_x}$ denotes the state vector consisting of positions and velocities, $u_i \in \mathcal{U}_i \subset \mathbb{R}^{n_u}$ is the control input vector, n_x and n_u represent the dimension of the state vector and the control input vector, respectively, and \mathcal{X}_i and \mathcal{U}_i are the state and control space of the i th object, respectively. In the discrete-time model, k means the k th time step for the objects. f_i and g_i are the nonlinear continuous-time and discrete-time dynamics models of the i th object. We consider the Gaussian process noise of velocity in the objects model, i.e., $\omega_i \sim \mathcal{N}(0, W_i)$ with a diagonal covariance matrix W_i . In the following, we use the discrete-time dynamics model to illustrate our approach.

2) *Collision Chance Constraints*: According to the previous introduction of velocity obstacles, we can obtain the collision condition of the object i with respect to the object j , which is defined as

$$v_i^k \notin \mathbb{V}_i \quad \text{or} \quad v_j^k \notin \mathbb{C}_i. \quad (10)$$

Since there is additional noise on the velocity of objects, the velocity of each object can be described as random variables $v_i^k := \hat{v}_i^k + \omega_i^k \sim \mathcal{N}(\hat{v}_i^k, W_i)$, where \hat{v}_i^k is the mean of the velocity and ω_i^k is the additional noise at time k . Hence, the collision avoidance constraints can be described in a probabilistic manner, where for each object i , the chance constraints can be expressed as

$$\Pr(v_i^k \notin \mathbb{V}_i) \geq 1 - \delta_i, \quad \forall i \in \mathbb{N}_n \quad (11a)$$

$$\text{or} \quad \Pr(v_j^k \notin \mathbb{C}_i) \geq 1 - \delta_i, \quad \forall i \in \mathbb{N}_n, \quad (11b)$$

where δ_i is the probability threshold of the collision risk.

B. Distributed Collision Avoidance Problem

Here, we formulate a distributed collision avoidance problem. For each object $i \in \mathbb{N}_n$, we formulate a discrete-time chance constrained optimization problem on N prediction steps with a sampling time Δt .

Problem 1: (Optimization with Probabilistic Chance Constraints) For each host object i , the position of the other objects $p_j, \forall j \in \mathbb{N}_n, j \neq i$, the initial state x_i^0 with uncertain noise, the reference state vector $x_{\text{ref},i}$ and the collision probability threshold δ_i have been provided. The objective is to compute

the optimal trajectories and control inputs for all of the objects. Thus, these objects can move from their initial states to the target states while maintaining the collision probability below the given threshold. The problem is defined as

$$\begin{aligned}
& \min_{x_i^1:N, u_i^0:N-1} \sum_{k=0}^{N-1} \|x_i^k - x_{\text{ref},i}^k\|_{Q_i} + \|u_i^k\|_{R_i} \\
& \text{subject to } x_i^{k+1} = g_i(x_i^k, u_i^k) + \omega_i^k \\
& v_i^{k+1} \sim \mathcal{N}(\hat{v}_i^{k+1}, W_i) \\
& \Pr(v_i^{k+1} \notin \mathbb{V}_i^{k+1}) \geq 1 - \delta_i, \quad \forall i \in \mathbb{N}_n \\
& \underline{x}_i^{k+1} \leq x_i^{k+1} \leq \bar{x}_i^{k+1} \\
& \underline{u}_i^k \leq u_i^k \leq \bar{u}_i^k \\
& x_i^{k+1} \in \mathcal{X}_i, \quad u_i^k \in \mathcal{U}_i,
\end{aligned} \tag{12}$$

where $\|x_i^k - x_{\text{ref},i}^k\|_{Q_i} = \langle (x_i^k - x_{\text{ref},i}^k), Q_i(x_i^k - x_{\text{ref},i}^k) \rangle$, $\|u_i^k\|_{R_i} = \langle u_i^k, R_i u_i^k \rangle$, Q_i and R_i are weighting matrices to penalize the deviation from the reference states and the unnecessary large control inputs, respectively. $\underline{x}_i, \bar{x}_i, \underline{u}_i, \bar{u}_i$ are the lower bound and upper bound of state variables and control inputs.

Remark 1: In the problem formulation (12), the collision avoidance constraints are based on the $(k+1)$ th time step. But in the next mathematical transformation, our discussion is based on the k th time step for simplicity.

IV. RECEDING HORIZON OPTIMIZATION PROBLEM WITH CHANCE CONSTRAINTS

The chance constraints of velocity obstacles $\Pr(v_i^k \notin \mathbb{V}_i^k) \geq 1 - \delta_i, \forall i \in \mathbb{N}_n$ mean that the risk of collision should be less than δ_i ; however, it is hard to determine it. Therefore, we need to do some mathematical manipulations to make it much easier to solve. The composite collision cone \mathbb{C}_i^k and velocity obstacles \mathbb{V}_i^k are the union of \mathbb{C}_{ij}^k and \mathbb{V}_{ij}^k with respect to object j with $j \neq i$. Thus, we start to analyze it in terms of one collision cone \mathbb{C}_{ij}^k or one velocity obstacle \mathbb{V}_{ij}^k . All of the pertinent variables and their relationships are demonstrated in Fig. 2.

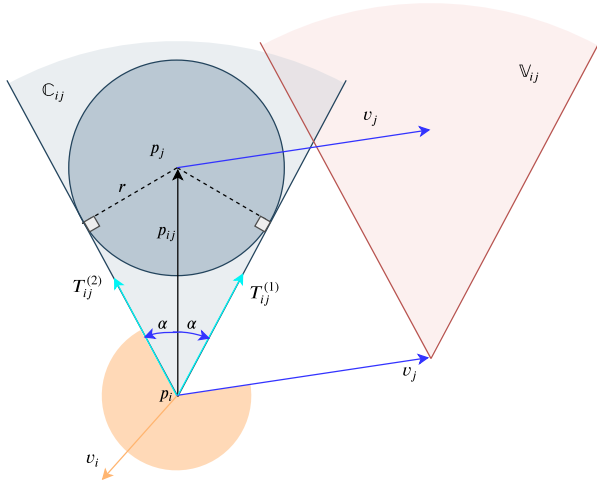


Fig. 2. Feasible region analysis based on the velocity obstacle \mathbb{V}_{ij}

Define the vector $p_{ij}^k := p_j^k - p_i^k \in \mathbb{R}^{n_p}$, where n_p is the dimension of the position vector, and the radius of the circle is given by $r = r_i + r_j$. Then, the angle between p_{ij}^k and the boundary line of the collision cone is the angle α_{ij}^k , as shown in Fig. 2. Obviously, $\sin \alpha_{ij}^k = \frac{r}{|p_{ij}^k|}$, and $\cos \alpha_{ij}^k = \sqrt{1 - \sin^2 \alpha_{ij}^k} = \frac{\sqrt{|p_{ij}^k|^2 - r^2}}{|p_{ij}^k|}$. Based on the rotation relationship of the vector p_{ij}^k , we can obtain the two tangent directional vectors $T_{ij,1}^k$ and $T_{ij,2}^k$, where

$$\begin{aligned}
T_{ij,1}^k &= \begin{bmatrix} \cos \alpha_{ij}^k & \sin \alpha_{ij}^k \\ -\sin \alpha_{ij}^k & \cos \alpha_{ij}^k \end{bmatrix} p_{ij}^k \\
T_{ij,2}^k &= \begin{bmatrix} \cos \alpha_{ij}^k & -\sin \alpha_{ij}^k \\ \sin \alpha_{ij}^k & \cos \alpha_{ij}^k \end{bmatrix} p_{ij}^k.
\end{aligned} \tag{13}$$

A. Analysis on Velocity Obstacles

Based on the velocity obstacle \mathbb{V}_{ij}^k , if the collision avoidance condition $v_i^k \cap \mathbb{V}_{ij}^k = \emptyset$ is satisfied, the feasible region of v_i^k should be the orange region shown in Fig. 2, according to the direction of v_j^k shown as the blue arrow. Obviously, different directions of v_j^k can result in different feasible regions of v_i^k . Therefore, we need to discuss it in terms of different cases, as shown in Fig. 3.

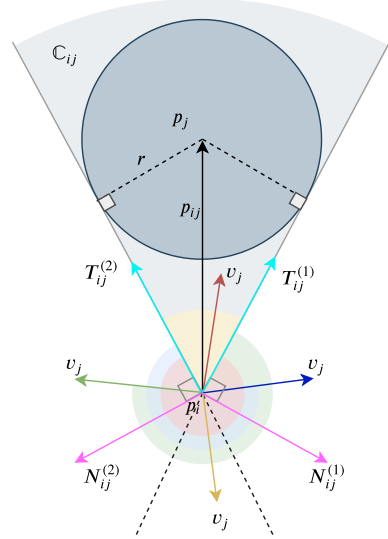


Fig. 3. Feasible region analysis for v_i^k according to v_j^k

- Case 1: $a > 0, b > 0$

Here, v_j^k is inside the collision cone \mathbb{C}_{ij}^k , which is shown as the red arrow in Fig. 3. The feasible region of v_i^k is shown as the red region, which means

$$v_i^k = cT_{ij,1}^k + dT_{ij,2}^k, \quad \neg(c > 0, d > 0), \tag{14}$$

where \neg represents the logical negation operation.

- Case 2: $a \leq 0, b \leq 0$

In this case, v_j^k is inside the inverted cone of \mathbb{C}_{ij}^k , which is shown as the yellow arrow in Fig. 3. The feasible region of v_i^k is in the yellow region, which means

$$v_i^k = cT_{ij,1}^k + dT_{ij,2}^k, \quad (c > 0, d > 0). \tag{15}$$

- Case 3: $a < 0, b > 0$

In this case, v_j^k is shown as the green arrow in Fig. 3, so we have

$$v_i^k = cT_{ij,1}^k + ev_j^k, \quad \neg(c > 0, e > 0). \quad (16)$$

- Case 4: $a > 0, b < 0$

Here, v_j^k is shown as the blue arrow in Fig. 3.

$$v_i^k = dT_{ij,2}^k + ev_j^k, \quad \neg(d > 0, e > 0). \quad (17)$$

To summarize all the scenarios as discussed above, let $v_i^k = aT_{ij,1}^k + bT_{ij,2}^k$, where $a, b \in \mathbb{R}$, and assume $v_i^k = cT_{ij,1}^k + dT_{ij,2}^k + ev_j^k$, then we have the following condition:

$$\begin{cases} e = 0, \neg(c > 0, d > 0), & \text{if } a > 0, b > 0 \\ e = 0, (c > 0, d > 0), & \text{if } a \leq 0, b \leq 0 \\ d = 0, \neg(c > 0, e > 0), & \text{if } a < 0, b > 0 \\ c = 0, \neg(d > 0, e > 0), & \text{if } a > 0, b < 0. \end{cases} \quad (18)$$

This condition is a case-by-case discussion about v_i^k according to the direction of v_j^k and there are logical negation operations in the condition, whereby it is sectionally discontinuous and disjunctive, which is hard to compute.

B. Analysis on Collision Cones

In this part, we focus on the relationship between the relative velocity v_{ij}^k and the collision cone \mathcal{C}_{ij}^k , as shown in Fig. 4. In order to meet the collision-free requirement, i.e., there is no intersection between the relative velocity v_{ij}^k and the collision cone \mathcal{C}_{ij}^k , v_{ij}^k should point outside the collision cone, which means that the angle between the two outer normal vectors $N_{ij,1}^k, N_{ij,2}^k$, and v_{ij}^k should be within the range $(-\frac{\pi}{2}, \frac{\pi}{2})$, as shown in Fig. 4.

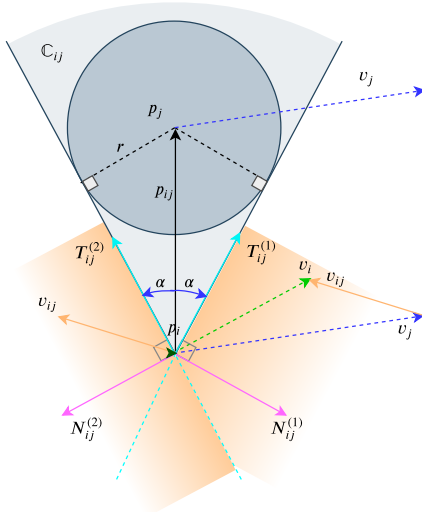


Fig. 4. Collision avoidance conditions analysis for v_{ij}^k

Two outer normal vectors $N_{ij,1}^k, N_{ij,2}^k$ are given by

$$\begin{aligned} N_{ij,1}^k &= \begin{bmatrix} \cos \frac{\pi}{2} & \sin \frac{\pi}{2} \\ -\sin \frac{\pi}{2} & \cos \frac{\pi}{2} \end{bmatrix} T_{ij,1}^k \\ N_{ij,2}^k &= \begin{bmatrix} \cos \frac{\pi}{2} & -\sin \frac{\pi}{2} \\ \sin \frac{\pi}{2} & \cos \frac{\pi}{2} \end{bmatrix} T_{ij,2}^k. \end{aligned} \quad (19)$$

The probabilistic condition of collision avoidance (11b) can be transformed as

$$\left(v_{ij}^k \cdot N_{ij,1}^k > 0 \right) \cup \left(v_{ij}^k \cdot N_{ij,2}^k > 0 \right), \quad \forall j \in \mathbb{N}_n, j \neq i. \quad (20)$$

In addition, chance constraints can be rewritten as

$$\begin{aligned} & \Pr \left(\left(N_{ij,1}^k \cdot v_{ij}^k > 0 \right) \cup \left(N_{ij,2}^k \cdot v_{ij}^k > 0 \right) \right) \geq 1 - \delta_{ij} \\ \Leftrightarrow & \Pr \left(\left(N_{ij,1}^k \cdot v_{ij}^k \leq 0 \right) \cup \left(N_{ij,2}^k \cdot v_{ij}^k \leq 0 \right) \right) \leq \delta_{ij} \\ \Leftrightarrow & \Pr \left(N_{ij,1}^k \cdot v_{ij}^k \leq 0 \right) \leq \delta_{ij,1}, \\ & \Pr \left(N_{ij,2}^k \cdot v_{ij}^k \leq 0 \right) \leq \delta_{ij,2} \\ \Leftrightarrow & \Pr \left(N_{ij,1}^{kT} v_i^k \leq N_{ij,1}^{kT} v_j^k \right) \leq \delta_{ij,1}, \\ & \Pr \left(N_{ij,2}^{kT} v_i^k \leq N_{ij,2}^{kT} v_j^k \right) \leq \delta_{ij,2}. \end{aligned} \quad (21)$$

Due to the existence of noise, v_{ij}^k is subject to a normal distribution, then we have

$$\delta_{ij,1} \delta_{ij,2} = \delta_{ij}. \quad (22)$$

In order to compute probabilistic chance constraints in a deterministic manner, we introduce the following lemma.

Lemma 1: Given any matrix A and scalar b , for a multivariate random variable $X(t)$ corresponding to the mean $\mu(t)$ and covariance $\Sigma(t)$, the chance constraint

$$\Pr(A^T X(t) < b) \leq \varphi, \quad (23)$$

is equivalent to a deterministic linear constraint

$$A^T \mu(t) - b \geq \eta, \quad (24)$$

where $\eta = \sqrt{2A^T \Sigma(t) A} \operatorname{erf}^{-1}(1 - 2\varphi)$, erf is the error function $\operatorname{erf}(x) = \frac{2}{\sqrt{\pi}} \int_0^x \exp(-t^2) dt$, and φ is the predefined allowable probability threshold of collision.

Notice that the variable v_i^k is a multivariate Gaussian random variable $v_i^k \sim N(\hat{v}_i^k, W_i)$, we can obtain the equivalent constraint:

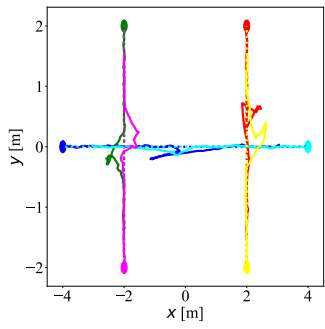
$$\begin{aligned} & \Pr \left(N_{ij,1}^{kT} v_i^k \leq N_{ij,1}^{kT} v_j^k \right) \leq \delta_{ij,1} \\ \Leftrightarrow & N_{ij,1}^{kT} \hat{v}_i^k - N_{ij,1}^{kT} v_j^k \geq \kappa_{ij,1} \\ & \Pr \left(N_{ij,2}^{kT} v_i^k \leq N_{ij,2}^{kT} v_j^k \right) \leq \delta_{ij,2} \\ \Leftrightarrow & N_{ij,2}^{kT} \hat{v}_i^k - N_{ij,2}^{kT} v_j^k \geq \kappa_{ij,2}, \end{aligned} \quad (25)$$

where $\kappa_{ij,1} = \sqrt{2N_{ij,1}^{kT} W_i N_{ij,1}^k} \cdot \operatorname{erf}^{-1}(1 - 2\delta_{ij,1})$ and $\kappa_{ij,2} = \sqrt{2N_{ij,2}^{kT} W_i N_{ij,2}^k} \cdot \operatorname{erf}^{-1}(1 - 2\delta_{ij,2})$.

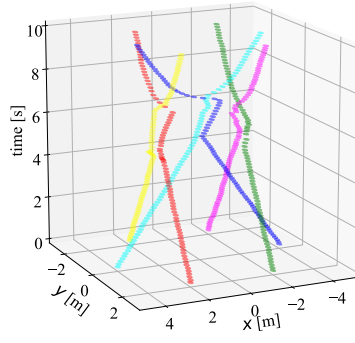
The calculations of $\kappa_{ij,1}$ and $\kappa_{ij,2}$ require the knowledge on W_i , i.e., the covariance of the i th robot at the current time. Moreover, the Kalman filter can be used to estimate the other objects velocity in the prediction horizon.

C. Deterministic MPC Formulation and Solving

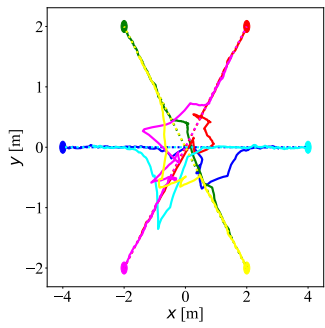
Problem 2: (MPC Problem with Deterministic Chance Constraints) The probabilistic chance constraints in (12) can be



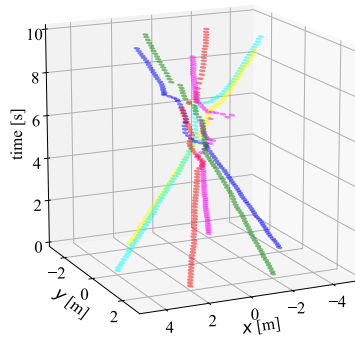
(a) 2D results of scenario 1



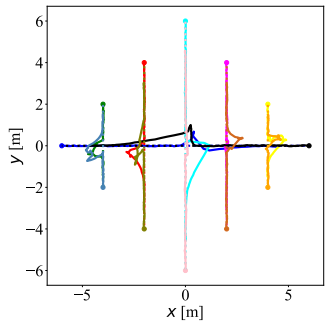
(b) 3D results of scenario 1



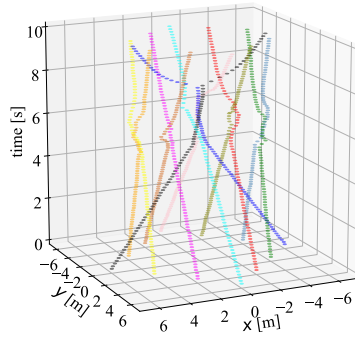
(c) 2D results of scenario 2



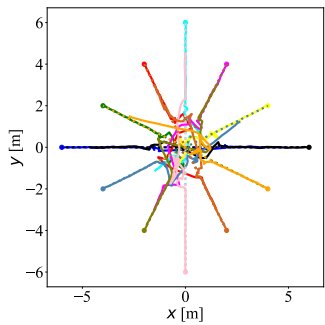
(d) 3D results of scenario 2



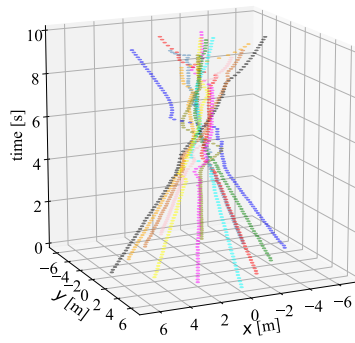
(e) 2D results of scenario 3



(f) 3D results of scenario 3



(g) 2D results of scenario 4



(h) 3D results of scenario 4

Fig. 5. Simulation results on multiple objects in different scenarios

transformed into a deterministic manner, which is tractable. This problem can be formulated as

$$\begin{aligned}
& \min_{x_i^1:N, u_i^0:N-1} \sum_{k=0}^{N-1} \left\| x_i^k - x_{\text{ref},i}^k \right\|_{Q_i} + \left\| u_i^k \right\|_{R_i} \\
& \text{subject to } x_i^{k+1} = f_i(x_i^k, u_i^k), \quad x_i^0 = p \\
& N_{ij,1}^{(k+1)T} \hat{v}_i^{k+1} - N_{ij,1}^{(k+1)T} v_j^{k+1} \geq \kappa_{ij,1}, \forall j \in \mathbb{N}_n, j \neq i \\
& N_{ij,2}^{(k+1)T} \hat{v}_i^{k+1} - N_{ij,2}^{(k+1)T} v_j^{k+1} \geq \kappa_{ij,2}, \forall j \in \mathbb{N}_n, j \neq i \\
& \underline{x}_i^{k+1} \leq x_i^{k+1} \leq \bar{x}_i^{k+1} \\
& \underline{u}_i^k \leq u_i^k \leq \bar{u}_i^k \\
& v_i^{k+1} \sim \mathcal{N}(\hat{v}_i^{k+1}, W_i) \\
& x_i^{k+1} \in \mathcal{X}_i, \quad u_i^k \in \mathcal{U}_i.
\end{aligned} \tag{26}$$

The collision probability between the host object i and all the other objects $j \in \mathbb{N}_n, j \neq i$ is less than a probability threshold δ_i , where

$$\delta_i = 1 - \prod_{j \in \mathbb{N}_n, j \neq i} (1 - \delta_{ij,1} \delta_{ij,2}). \tag{27}$$

At time t , the cost function is optimized under the constraints in (26) to obtain the optimal control sequence.

$$u_i^* = \left[(u_i^{*0})^T \quad (u_i^{*1})^T \quad \dots \quad (u_i^{*(N-1)})^T \right]^T, \tag{28}$$

and only the first control input u_i^{*0} will be executed. The pseudocode of how to address the velocity obstacle based receding horizon motion planning with chance constraints is shown in Algorithm 1.

V. RESULTS

This section describes the implementation of the proposed method, and the effectiveness of the method is evaluated by simulations. All the relevant parameters of the simulation are shown in Table II in the Appendix. Here, we add the Gaussian noise to the velocity of objects model, and the added measurement noise is zero mean with the covariance W_i . Taking the noisy measurements as inputs, a Kalman filter is employed to estimate the state of other moving objects. All of the simulations are implemented in Python 3.7 environment on a PC with Intel i5 CPU@3.30 GHz. The video demonstrating the results can be found at <https://www.youtube.com/watch?v=MwA6eUhlAw4>, and the source code is available at <https://github.com/Lisnol1/Velocity-Obstacle-Motion-Planning>.

Here, four different scenarios for 6 and 12 objects are designed for validation purposes, and the simulation results are shown in Fig. 5. Different colors represent different objects with radius r_i . In the simulation, the radius of all objects is set as $r_i = 0.2$ m. The circles in (b), (d), (f), and (h) of Fig. 5 demonstrate the approximate shape of objects. The solid lines and dotted lines in (a), (c), (e), and (g) of Fig. 5 represent the planned trajectories and reference trajectories for each object, respectively. The scenario 1 in Fig. 5 means that there are 6 objects whose target position is the symmetry point of the initial position along the x or y axis. For example, for the green object, its initial position is $(-2, 2)$ m and then its target

Algorithm 1 Velocity Obstacle Based Receding Horizon Motion Planning with Chance Constraints.

Initialization: Dynamic model for all agents; the agents number n_{num} ; the radius of agents r_i ; weighting matrices Q_i and R_i in the cost function; initial position and target position of all agents; reference positions of all agents; upper and lower bound of the state x and control input u , i.e., \bar{x}, \underline{x} and \bar{u}, \underline{u} , respectively; runtime of MPC r_{run} ; sampling time τ_s ; covariance matrix W_i ; threshold δ_1 and δ_2 . Set the time step $t = 0$.

while $t \leq r_{\text{run}}$ **do**

for $i \in \mathbb{N}_n$ **do**

for $k = 0, 1, \dots, N-1$ **do**

 Compute x_i^{k+1} for the i th agent based on x_i^k by using (9).

 Generate constraints of physical limitations for the i th agent.

 Compute the two transformed deterministic constraints for the i th agent by (25).

end for

 Compute the quadratic cost function for the i th agent.

 Solve the deterministic optimization problem (26).

 Obtain the optimal control sequence u_i^* .

 Execute the first control input u_i^{*0} for the i th agent.

 Pass the updated states of neighbors $j \in \mathbb{N}_n, j \neq i$ to the i th agent.

end for

$t = t + \tau_s$.

end while

position is $(-2, -2)$ m. Fig. 5(a) shows the trajectories of the 6 objects and Fig. 5(b) presents the position of all objects in each time step. According to Fig. 5(a) and (b), there is no collision happening in this scenario, as no two objects occur in the same position at the same time. The scenario 2 in Fig. 5 indicates that the 6 objects starting from their initial positions need to pass through the origin point $(0, 0)$ m without any collision and reach their target positions that are the symmetry points of the initial positions along with the origin, i.e., along the both x and y axis. To be specific, the green object in scenario 2 starts from $(-2, 2)$ m and needs to reach its target position $(2, -2)$ m. The results of the scenario 2 are shown in Fig. 5(c) and (d). Also, all objects are able to arrive at their destinations with no collision, based on the two subfigures. Similarly, the task in scenario 3 is to reach the target positions that are symmetry points along the x or y axis of the initial positions for all 12 objects. Fig. 5(e) and (f) illustrate the resulted trajectories of these 12 objects, and it is straightforward to observe that all of the 12 objects can reach their target positions without collisions. In scenario 4, there are 12 objects whose target positions are the symmetry points of the initial positions along with the origin, i.e., along the both x and y axis. The trajectories of these 12 objects are shown in Fig. 5(g) and (h), and we can observe that all of the trajectories are collision-free, which satisfies our requirement. Overall, all the subfigures from Fig. 5(a) to (h) indicate that this approach can effectively avoid collisions with the other

moving objects (including agents and obstacles, which can be represented by different dynamics and shapes).

The distances between each pair of objects in all scenarios are shown in Fig. 6. The subfigures from the first one to the fourth one are the results from scenario 1 to scenario 4, respectively. According to all these subfigures in Fig. 6, it is apparent that each object can maintain a certain safety distance from other objects, as the minimum safety distance is greater than 0.1 m, which is the radius of each object. Therefore, there is no collision happening in all of the four scenarios.

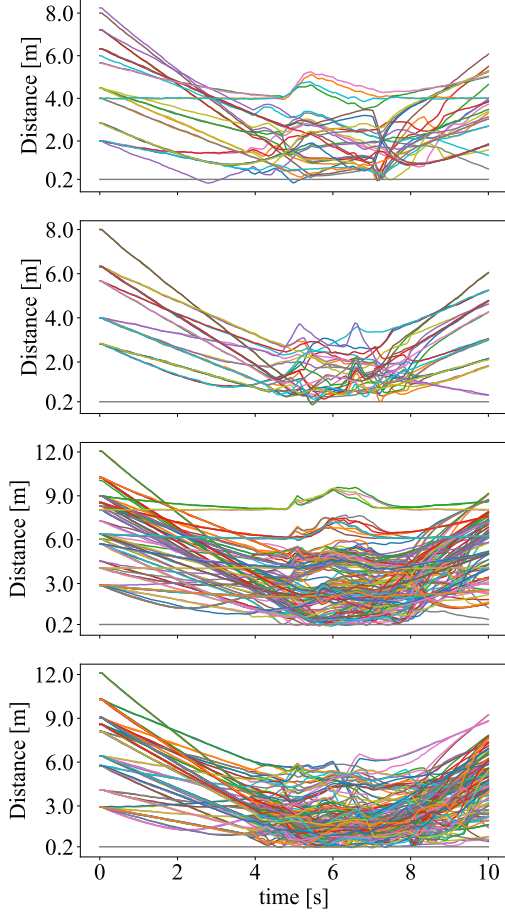


Fig. 6. Distance between each pair of objects in all scenarios

For scenario 4, we compare the results of our method under different three levels of measurement noise ($\frac{1}{4}W_i$, W_i , and $4W_i$) with the deterministic MPC method, which is proposed in [25]. The minimum distance between each pair of agents and the success rate are treated as the safety metrics. The comparison results are shown in Table I. Besides, due to a tighter bound of collision probability approximation, our method can keep a larger minimum distance during running under the same noise level, compared with the deterministic MPC method. Also, with a larger noise level, our proposed method maintains the success rate of 100%, but the success rate of deterministic MPC decreases from 71% to 41%. According to Table I, we can observe that our proposed method achieves higher safety performance compared with the deterministic MPC method.

TABLE I
TRAJECTORY SAFETY COMPARISON OF TWO ALGORITHMS WITH DIFFERENT LEVELS OF NOISE (THE VALUES ARE COMPUTED FROM SUCCESSFUL RUNS).

Noise	Safety metrics	Deterministic MPC [25]	Our method
$\frac{1}{4}W_i$	Minimum distance	0.112 m	0.167 m
	Success rate	72 %	100 %
W_i	Minimum distance	0.136 m	0.194 m
	Success rate	61 %	100 %
W_i	Minimum distance	0.148 m	0.231 m
	Success rate	41 %	100 %

Fig. 7 shows the computational time with an increasing number of agents moving across the origin circle. In this case, the initial positions and the target positions of all agents are symmetric along the origin, i.e., both the x and y axis. Based on Fig. 7, the computational time for different agent numbers are less than the sampling time $\tau_s = 0.05s$, which means that the real-time implementation can be realized. Besides, it is straightforward to observe that the computational time increases with the number of agents increasing.

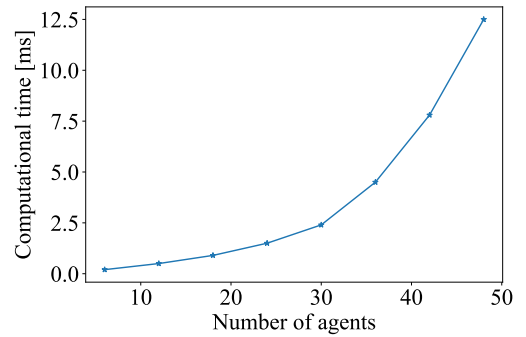


Fig. 7. Distance between each pair of objects in all scenarios

VI. CONCLUSION

In this paper, a velocity obstacle based receding horizon motion planning method, is proposed for potential collision avoidance. Based on the feasible region of v_i provided by the velocity obstacles method, a chance constrained RHC problem is formulated and solved. A feasible region of velocity for the host agent is derived and formulated as probabilistic collision constraints. Hence the proposed method can generate the trajectories at the velocity level. Besides, this method can also provide a probability threshold of potential collision during the motion planning process. Several simulation scenarios for multiple agents are employed to validate the effectiveness and efficiency of our proposed methodology. In terms of the future work, one prospective research is to realize the motion planning in 3-dimensional space. Moreover, another future work is to consider the uncertainty in shape and velocity of the agents at the same time.

APPENDIX

Table II shows the values of parameters in Section IV.

TABLE II
PARAMETER SETTING

Meaning	Notation	Value	Unit
Radius	r_i	0.1	m
Mass	m	1	kg
Covariance of noise	W_i	diag(0.01, 0.01, 0.05, 0.05)	-
Threshold	$\delta_{i,1}, \delta_{i,2}$	0.1, 0.1	-
Sampling time	Δt	0.05	s
Prediction horizon	N	25	-
State weighting matrix	Q_i	diag(10, 10, 1, 1)	-
Control input weighting matrix	R_i	diag(1, 1)	-
Maximum/minimum state limitations	$\bar{x}_i/\underline{x}_i$	$[\infty \ \infty \ 10 \ 10]^T / [-\infty \ -\infty \ -10 \ -10]^T$	-
Maximum/minimum input limitations	$\bar{u}_i/\underline{u}_i$	$[\infty \ \infty]^T / [-\infty \ -\infty]^T$	-

REFERENCES

- [1] T. Gu, J. Atwood, C. Dong, J. M. Dolan, and J.-W. Lee, "Tunable and stable real-time trajectory planning for urban autonomous driving," in *2015 IEEE/RSJ International Conference on Intelligent Robots and Systems (IROS)*. IEEE, 2015, pp. 250–256.
- [2] P. Hang, S. Huang, X. Chen, and K. K. Tan, "Path planning of collision avoidance for unmanned ground vehicles: A nonlinear model predictive control approach," *Proceedings of the Institution of Mechanical Engineers, Part I: Journal of Systems and Control Engineering*, vol. 235, no. 2, pp. 222–236, 2021.
- [3] P. Fiorini and Z. Shiller, "Motion planning in dynamic environments using velocity obstacles," *The International Journal of Robotics Research*, vol. 17, no. 7, pp. 760–772, 1998.
- [4] J. A. Douthwaite, S. Zhao, and L. S. Mihaylova, "Velocity obstacle approaches for multi-agent collision avoidance," *Unmanned Systems*, vol. 7, no. 01, pp. 55–64, 2019.
- [5] J. Van den Berg, M. Lin, and D. Manocha, "Reciprocal velocity obstacles for real-time multi-agent navigation," in *2008 IEEE International Conference on Robotics and Automation*. IEEE, 2008, pp. 1928–1935.
- [6] J. Van Den Berg, J. Snape, S. J. Guy, and D. Manocha, "Reciprocal collision avoidance with acceleration-velocity obstacles," in *2011 IEEE International Conference on Robotics and Automation*. IEEE, 2011, pp. 3475–3482.
- [7] D. Wilkie, J. Van Den Berg, and D. Manocha, "Generalized velocity obstacles," in *2009 IEEE/RSJ International Conference on Intelligent Robots and Systems*. IEEE, 2009, pp. 5573–5578.
- [8] J. Snape, J. Van Den Berg, S. J. Guy, and D. Manocha, "The hybrid reciprocal velocity obstacle," *IEEE Transactions on Robotics*, vol. 27, no. 4, pp. 696–706, 2011.
- [9] J. Ji, A. Khajepour, W. W. Melek, and Y. Huang, "Path planning and tracking for vehicle collision avoidance based on model predictive control with multiconstraints," *IEEE Transactions on Vehicular Technology*, vol. 66, no. 2, pp. 952–964, 2016.
- [10] X. Zhang, J. Ma, Z. Cheng, F. L. Lewis, and T. H. Lee, "Sequential convex programming for collaboration of connected and automated vehicles," *arXiv preprint arXiv:2101.00202*, 2021.
- [11] Z. Cheng, J. Ma, X. Zhang, C. W. de Silva, and T. H. Lee, "ADMM-based parallel optimization for multi-agent collision-free model predictive control," *arXiv preprint arXiv:2101.09894*, 2021.
- [12] X. Zhang, J. Ma, Z. Cheng, S. Huang, C. W. de Silva, and T. H. Lee, "Accelerated hierarchical ADMM for nonconvex optimization in multi-agent decision making," *arXiv preprint arXiv:2011.00463*, 2020.
- [13] M. Defoort, A. Doniec, and N. Bouraqadi, "Decentralized robust collision avoidance based on receding horizon planning and potential field for multi-robots systems," in *Informatics in Control Automation and Robotics*. Springer, 2011, pp. 201–215.
- [14] H. Cheng, Q. Zhu, Z. Liu, T. Xu, and L. Lin, "Decentralized navigation of multiple agents based on ORCA and model predictive control," in *2017 IEEE/RSJ International Conference on Intelligent Robots and Systems (IROS)*. IEEE, 2017, pp. 3446–3451.
- [15] X. Zhang, J. Ma, S. Huang, Z. Cheng, and T. H. Lee, "Integrated planning and control for collision-free trajectory generation in 3d environment with obstacles," in *2019 19th International Conference on Control, Automation and Systems (ICCAS)*. IEEE, 2019, pp. 974–979.
- [16] C. E. Luis and A. P. Schoellig, "Trajectory generation for multiagent point-to-point transitions via distributed model predictive control," *IEEE Robotics and Automation Letters*, vol. 4, no. 2, pp. 375–382, 2019.
- [17] H. Zhu and J. Alonso-Mora, "Chance-constrained collision avoidance for mavs in dynamic environments," *IEEE Robotics and Automation Letters*, vol. 4, no. 2, pp. 776–783, 2019.
- [18] M. da Silva Arantes, C. F. M. Toledo, B. C. Williams, and M. Ono, "Collision-free encoding for chance-constrained nonconvex path planning," *IEEE Transactions on Robotics*, vol. 35, no. 2, pp. 433–448, 2019.
- [19] J. Ma, Z. Cheng, X. Zhang, A. A. Mamun, C. W. de Silva, and T. H. Lee, "Data-driven predictive control for multi-agent decision making with chance constraints," *arXiv preprint arXiv:2011.03213*, 2020.
- [20] J. Ma, Z. Cheng, X. Zhang, M. Tomizuka, and T. H. Lee, "Optimal decentralized control for uncertain systems by symmetric Gauss-Seidel semi-proximal ALM," *IEEE Transactions on Automatic Control*, 2021.
- [21] L. Blackmore, H. Li, and B. Williams, "A probabilistic approach to optimal robust path planning with obstacles," in *2006 American Control Conference*. IEEE, 2006, pp. 2831–2837.
- [22] X. Zhang, J. Ma, Z. Cheng, S. Huang, S. S. Ge, and T. H. Lee, "Trajectory generation by chance-constrained nonlinear mpc with probabilistic prediction," *IEEE Transactions on Cybernetics*, 2020.
- [23] L. Blackmore, M. Ono, and B. C. Williams, "Chance-constrained optimal path planning with obstacles," *IEEE Transactions on Robotics*, vol. 27, no. 6, pp. 1080–1094, 2011.
- [24] D. Lenz, T. Kessler, and A. Knoll, "Stochastic model predictive controller with chance constraints for comfortable and safe driving behavior of autonomous vehicles," in *2015 IEEE Intelligent Vehicles Symposium (IV)*. IEEE, 2015, pp. 292–297.
- [25] T. Nageli, L. Meier, A. Domahidi, J. Alonso-Mora, and O. Hilliges, "Real-time planning for automated multi-view drone cinematography," *ACM Transactions on Graphics (TOG)*, vol. 36, no. 4, pp. 1–10, 2017.